

# The influence of a phase change on the thermal history of a sample undergoing laser irradiation

T.W. WOJTATOWICZ, K. ROŻNIAKOWSKI

*Institute of Physics, Technical University of Lodz, Wolczanska 219, 93-005 Lodz, Poland*

L. WOJTCZAK

*Department of Solid State Physics, University of Lodz, Pomorska 149/153, 90-236 Lodz, Poland*

This paper presents a comparison of the shapes of the thermal history curves for the rear surface of a sample undergoing laser irradiation. The curves are obtained experimentally and also calculated using the quasi-implicit technique of finite differences. The position and the size of the plateau observed on the theoretical and experimental curves has a significant impact on the accuracy of the determination of the thermal diffusivity obtained using the axial laser flash method. The experimental measurements were performed on phase-change composite materials and also on moist porous material samples (a gypsum slurry).

## 1. Introduction

As a result of the absorption of pulsed laser radiation (with a square cross-section in time and space and with appropriate parameters) by the subsurface material, a surface heat source is generated (Fig. 1). To a first approximation the sample can be regarded as an infinite plate (with axial symmetry) limited by the thermally insulated surfaces at  $x = 0$  and  $x = L$  with the thickness of the absorbing layer  $h$  being infinitesimal.

In this case (in the absence of heat sources in the sample volume) the thermal conduction under non-equilibrium thermal conditions can be described as;

$$\nabla^2 T(x, r, \varphi, t) = \frac{1}{\alpha} \frac{\partial T}{\partial t} \quad (1)$$

where  $\alpha$  is the thermal diffusivity, and  $x, r, \varphi$  are the cylindrical co-ordinates of the point at which the temperature  $T$  is determined at a time  $t$ .

Only metals satisfy the ideal conditions presented above. For other materials (especially composite materials on which this paper will concentrate) we must take into consideration the finite thickness of the heat source  $h$ , and in this case the thermal conduction equation for heat sources in the sample volume is;

$$\nabla^2 T(x, r, \varphi, t) = \frac{1}{\alpha} \frac{\partial T}{\partial t} + \frac{q}{\lambda} \quad (2)$$

where  $\lambda$  is the thermal conductivity and  $q$  is the heat flux generated in the material.

The heat pulse measured after it has passed through the irradiated sample contains information on the thermophysical properties of the material. The temperature changes on the rear surface, i.e., the surface opposite to the one absorbing the laser radiation,

called the thermal history (TH), are the basis for determining the thermal diffusivity. This concept is applied in the laser flash method for thermal diffusivity measurements [1].

The standard algorithm to calculate the thermal diffusivity is based on the following equation [1] which is obtained from the solution of Equation 1:

$$\alpha = 0.139 \frac{L^2}{t_{0.5}} \quad (3)$$

where  $t_{0.5}$  is the time delay until the temperature of the rear surface reaches one half of the maximum temperature increase  $T_{\max}$  after the front surface is heated by the laser pulse and  $L$  is the sample thickness. The shape of the thermal history for an ideal case, calculated using a non-dimensional temperature  $\Theta = T/T_{\max}$  and a non-dimensional time  $\omega = t/t_{0.5}$ , is presented in Fig. 2.

The most important problem in our case is a phase change produced by the heat absorption, and the existence of a moving surface of separation between the two phases. The only simple exact solution in cylindrical co-ordinates corresponds to the supply or removal of heat by a continuous line source [2]. For a region externally bound by a circular cylinder with constant surface temperatures only an approximate solution is available. To solve more complex problems we must use numerical methods.

The use of numerical methods has advantages, such as the point that the variation in the thermal properties with temperature, which are usually considerable over the temperature ranges involved in melting and solidification, can be taken into account.

When a heat pulse moves across a material, if a phase change takes place (e.g., the melting of ice or

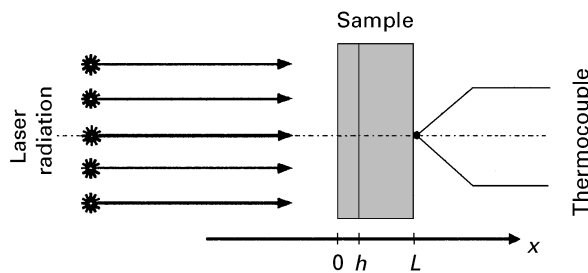


Figure 1 The geometry of the sample irradiation (back view).

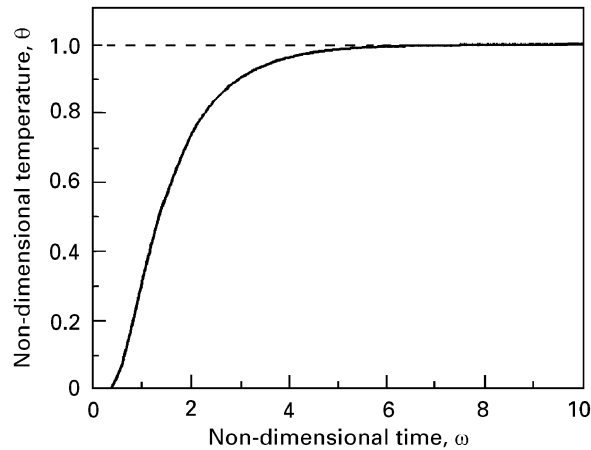


Figure 2 The ideal shape of the thermal history.

the vapourization of water in pores), the heat conduction equation, Equation 2, must be solved with the following boundary conditions [2]:

$$T_1(x) = T_2(x) = T_p \quad (4)$$

$$\lambda_1 \frac{\partial T_1}{\partial x} - \lambda_2 \frac{\partial T_2}{\partial x} = H_v \rho \frac{dx}{dt} \quad (5)$$

The first condition, Equation 4, means that the temperature  $T_1$  of first phase (e.g., ice) and the temperature  $T_2$  of the second phase (e.g., water) at points  $x$  lying on the surface of separation between the two phases must be equal to the temperature  $T_p$  at which the phase change occurs. Since the surface of separation is moving along with the heat pulse, then the second condition, Equation 5, concerns the absorption of the latent heat of fusion  $H_v$  occurring when the surface of separation moves a distance  $dx$  during time  $dt$  (the subscripts indicate the different phases).

The phase change should not only affect the thermal conduction equation, but also be reflected in the shape of the TH plot. In this paper, we present a comparison of TH shapes obtained experimentally with those calculated using a quasi-implicit technique.

The measurements were performed on phase-change composite materials (PCM) [3, 4] and also on moist porous material samples (a gypsum slurry). Composite materials containing a substance with a phase-change within the range 18–50 °C, such as a fatty acid finds application as solar heat storage layers in the outside walls of a building.

## 2. Experimental procedure

The thermal history was recorded with an experimental set-up that is shown schematically in Fig. 3

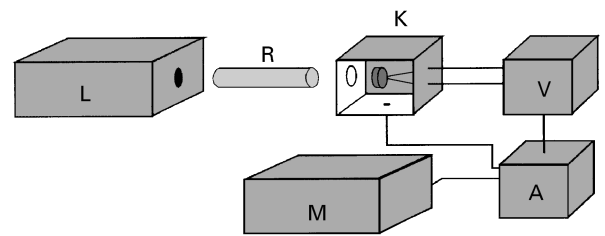


Figure 3 A schematic diagram of the experimental apparatus.

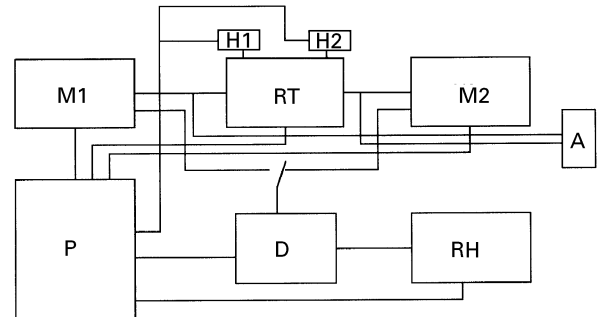


Figure 4 A schematic diagram of the measurement circuit and temperature control mechanism.

and that consists of a pulsed laser L (R is radiation pulse) a special chamber K, in which the sample in the form of a disk (of thickness of a few millimeters and diameter equal to the laser beam diameter) is placed and a sensitive small temperature rise measurement channel V-A [5] controlled by the microcomputer M. Fig. 4 presents the circuit with which the temperature of the chamber (M1) and sample (M2) is measured using semiconductor thermometers and controlled by the controller RT (H1 is the heater and H2 is the cooler), the air's relative humidity is measured by the sensor RH, and the measured values are presented on display D and sent to the computer (P is the power supply). The moisture content in the sample was measured after the measurement of the TH with the aid of an Ohaus MB200 moisture determination balance. The energy and duration of the laser pulse must be chosen so as to heat the sample above the phase-change point without evaporating the sample's front surface.

## 3. Modelling of the influence of the phase change

The disk-shaped samples absorb the laser radiation in such a manner, that within the material a quasivolume heat source is produced, as is described by Equation 2. The simplest method of evaluating this equation is the finite differences method [6]. In this method the temperature  $T^{(t+\Delta t)}$  of any point at a time  $t + \Delta t$  can be obtained from the temperature  $T^{(t)}$  at time  $t$  of that point and its four nearest neighbours. The method constrains  $\Delta t$  to a very small value, which results in long computation times and excessive round-off errors which negate the advantage of the simplicity of this method.

We can apply the quasi-implicit technique [7], in which the first step is the same as that in the ordinary technique but in a second step we calculate the

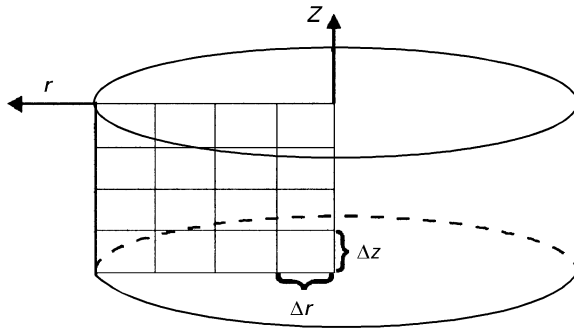


Figure 5 Division of the sample into toroidal elements.

temperature  $T^{(t)}$  at time  $t$  on the basis of the temperature  $T^{(t+\Delta t)}$  by the time reversal process and add the amendment to the temperature  $T^{(t+\Delta t)}$  at the end.

It is easiest to introduce a matrix formalism, in which the temperatures of a sample's volume elements are represented by the matrix  $T$ . Fig. 5 shows such volume elements with a constant thickness  $\Delta r$  and a height  $\Delta z$  and with an increasing radius  $r$ .

The absorption of laser light (according to Bougers' law) is described by an absorption matrix  $A$ , while for heat transfer two matrices are defined: the radial thermal diffusion matrix  $R$  and the vertical thermal diffusion matrix  $Z$ . The latent heat of fusion is represented by the temperature equivalent of the latent heat of fusion matrix  $H$ .

The radial thermal diffusion matrix  $R$  is defined as follows:

$R =$

$$\frac{\Delta t}{\Delta r^2} \begin{bmatrix} -2\alpha & \alpha^+(1) & & & & \\ \alpha^-(2) & -2\alpha & \alpha^+(2) & & & \\ & \dots & \dots & \dots & & \\ & & & -2\alpha & \alpha^+(n-1) & \\ & & & \alpha^-(n) & -2\alpha & \alpha^+(n) \end{bmatrix} \quad (6)$$

where:  $n =$  number of rows,  $i =$  the ordinal of a row  $\alpha^+(i) = \alpha i / i - 0.5$  and  $\alpha^-(i) = \alpha i - 1 / i - 0.5$ , and the vertical thermal diffusion matrix  $Z$  is:

$$Z = \frac{\Delta t}{\Delta z^2} \begin{bmatrix} -\alpha & \alpha & & & & \\ & \alpha & -2\alpha^2 & & & \\ & & & -2\alpha^2 & \alpha & \\ & & & \alpha & -2\alpha^2 & \\ & & & & & \dots \end{bmatrix} \quad (7)$$

TABLE I The parameters used in the calculations

Item	Symbol	Unit	Set 1	Set 2	Set 3
Radiation power	$P$	W	1000	2000	3000
Pulse duration	$t$	ms	4	4	4
Temperature rise to the phase-change point	$T_p$	K	28	28	2
Latent heat of fusion	$H_v$	kJ	70	70	70
Effective thermal conductivity	$\lambda_c$	$\text{W m}^{-1}\text{s}$	1.9	1.9	2.1
Specific heat	$C_p$	$\text{J kg}^{-1}\text{K}$	500	500	100

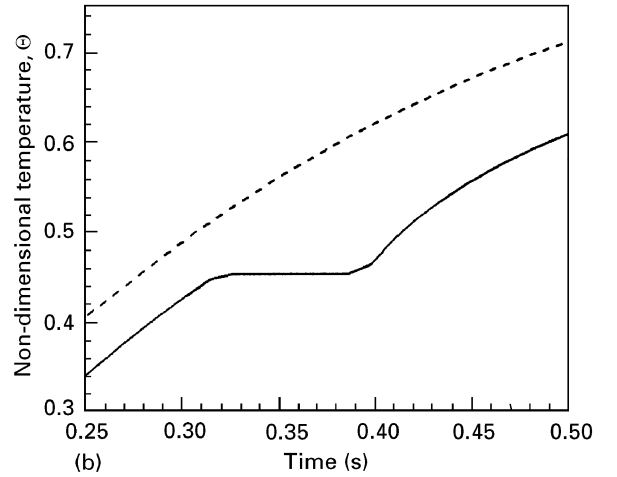
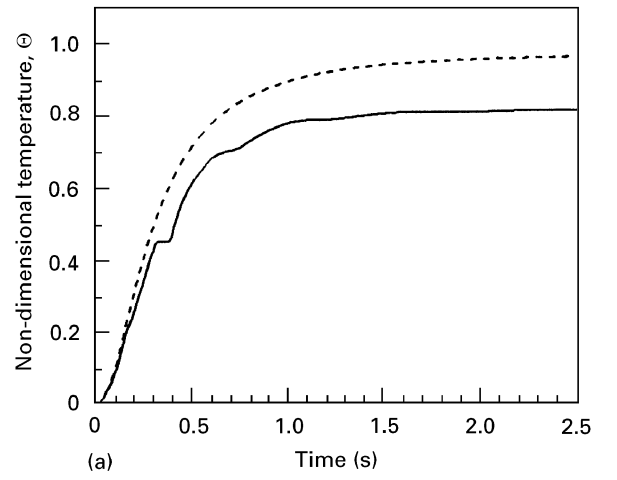


Figure 6 The thermal history with (solid line) and without (dotted line) a phase change for the first data set. (a) full shape and (b) enlarged fragment.

The temperature  $T^{(t+\Delta t)}$  of any point at time  $t + \Delta t$  can be obtained from the temperature  $T^{(t)}$  at time  $t$  with the aid of following equations:

$$T^{(t)} = A + T^{(t)} \quad (8)$$

$$T^{(t+\Delta t)} = T^{(t)} + \frac{1}{2} \left[ (Z + Z^2) T^{(t)} + 2ZT^{(t)}R + T^{(t)}(R + R^2) \right] \quad (9)$$

Then, we compare the thus obtained temperatures of all points at the phase-change temperature  $T_p$  and make the corrections using the algorithm described in reference [7].

For the gypsum slurry samples (with a diameter of 7 mm and a thickness of 3 mm) with its pores filled by paraffin (density  $2300 \text{ kg m}^{-3}$ ; the other effective parameters used in our calculations are presented in Table I. It should be noted that some of them are rough estimates based on data for paraffin published in the literature.) we calculated with the aid of the above technique the TH (using a non-dimensional temperature  $\Theta$ ) for a few sets of parameters. In the case where a phase-change occurs, we repeat the calculations using a temperature rise at the phase-change point higher than the maximum temperature rise previously obtained, in order to obtain

the TH without the phase-change at the same values of the parameters.

Fig. 6a (solid line) presents the TH plot obtained for the first set of parameters (Table I). The maximum temperature rise is less than that obtained when the phase-change does not occur (dotted line). An enlarged fragment (Fig. 6b) shows that a plateau occurs in the TH curve (the temperature of the rear surface is stable during the first 0.1 s, which does not appear under ideal conditions – see the TH shown on Fig. 2). Fig. 7 shows the TH plot obtained for the second and third parameter sets (the arrows point to the stable temperature fragments on the TH curve).

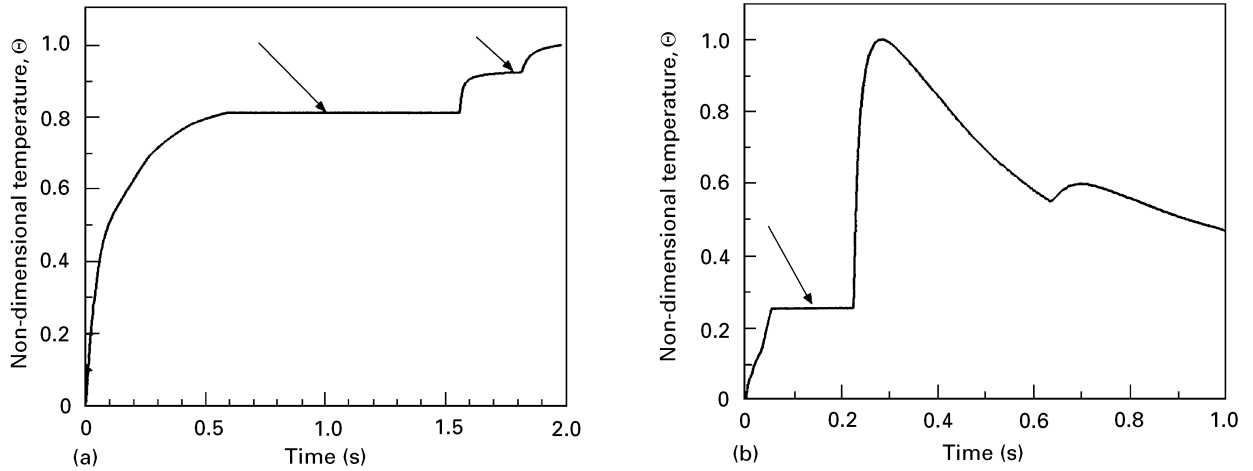


Figure 7 The thermal history with a phase change for the (a) second and (b) third data sets.

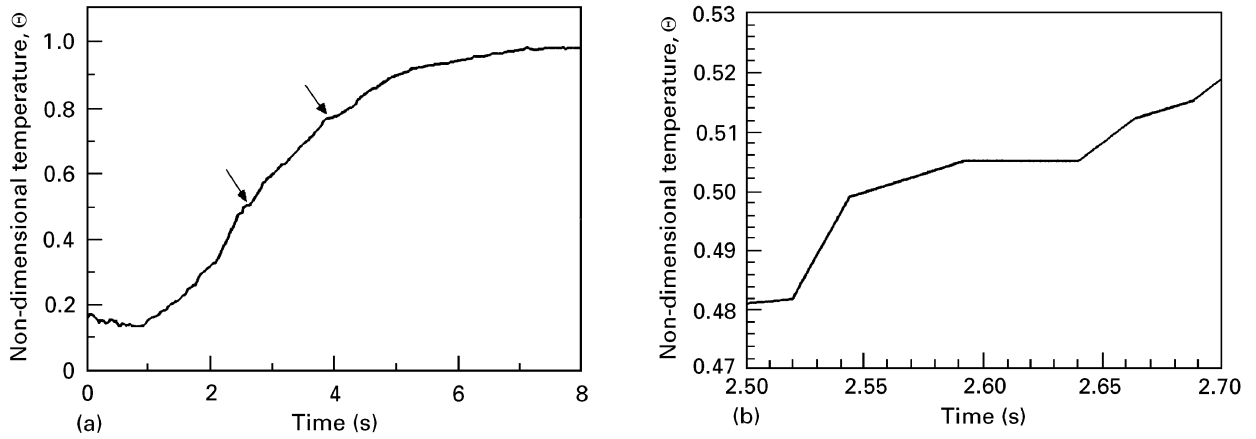


Figure 8 The thermal history for a gypsum slurry mixed with a fatty acid undergoing a phase change. (a) full shape and (b) enlarged fragment.

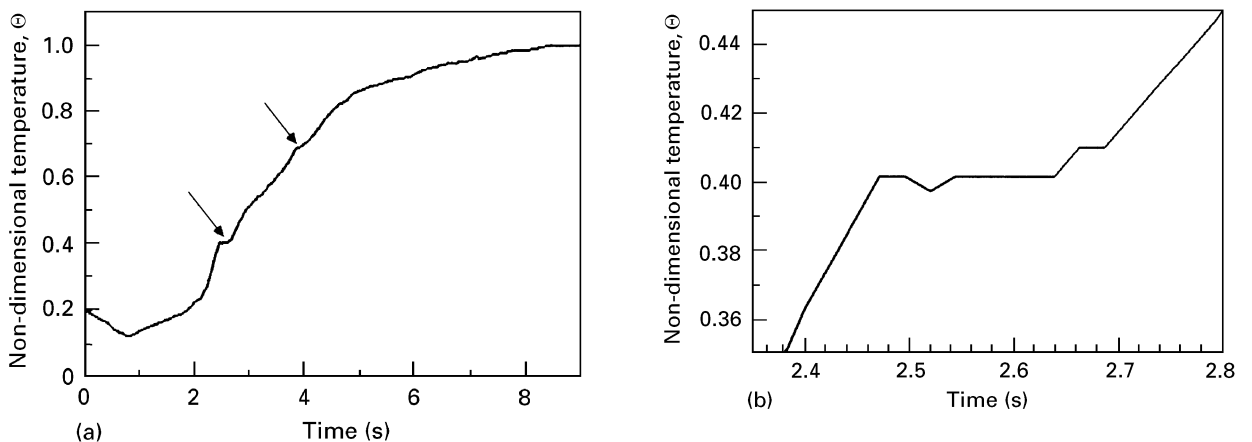


Figure 9 The thermal history for a gypsum slurry mixed with a fatty acid undergoing a phase change. (a) full shape and (b) enlarged fragment.

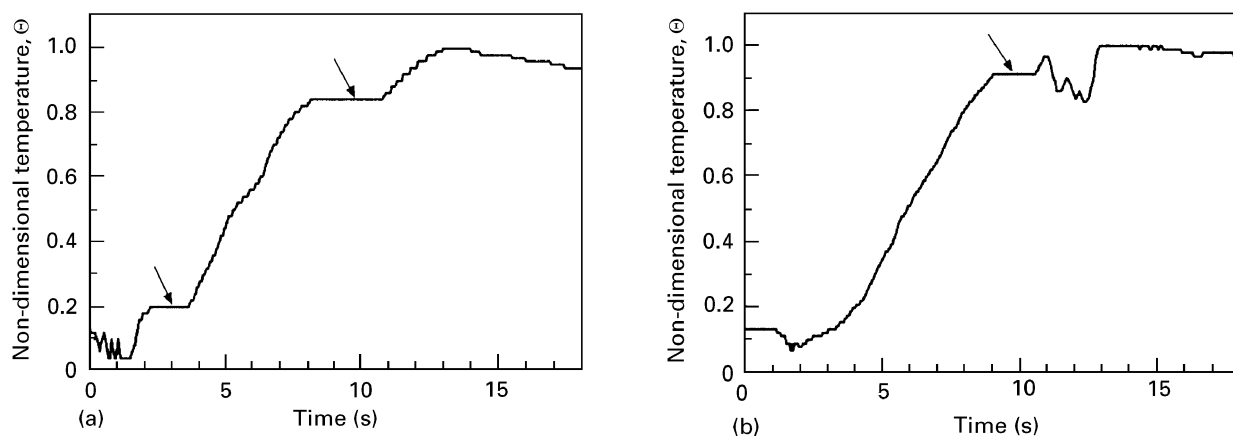


Figure 10 The thermal history plot for the moist gypsum slurry registered for an initial temperature of (a)  $-0.8^{\circ}\text{C}$  and (b)  $-1.9^{\circ}\text{C}$ .

#### 4. Experimental results

Using the experimental set-up described in Section 2 we recorded the TH of two PCM samples. The first sample was gypsum slurry mixed with fatty acids for inclusion in the gypsum pores with a weight ratio of gypsum (anhydrous), water and fatty acids equal to 1:0.8:0.5 (Fig. 8a) and the second sample had weight ratios of 1:0.8:0.8 (Fig. 9a). Enlarged fragments (Figs. 8b and 9b) show that a plateau occurs on the TH curves. The shapes are similar to those calculated from the first set of parameters and shown in Fig. 6.

A TH curve shaped in a similar manner to the theoretical one shown on Fig. 7a, was obtained for moist gypsum slurry samples (Fig. 10). The gypsum slurry samples were prepared in a weight ratio of gypsum and water of 1:0.8, and contained 30 wt% water. The initial temperature of the sample was near the water-ice phase change point, so that during the transfer of the heat pulse the ice inside the sample liquified. The processes that occur in this material during the measurements are highly complicated (e.g., the transfer of water in the pores), and hence the shapes of the TH curves are also very complex.

#### 5. Conclusions

The occurrence of a phase change during the transfer of a heat pulse mainly causes a reduction in the maximum temperature rise at the rear surface of the sample. Any influence on the time it takes for the maximum temperature to be reached is not clear. The position and the size of the plateau in a TH curve are significant factors in the accuracy of the determination of the time  $t_{0.5}$  and hence for the thermal diffusivity obtained from the axial laser flash method with the use of Equation 3.

One can minimize the error in the thermal diffusivities by use of a different analysis method that uses more than one or two characteristic points on a curve. Such a method is the least squares technique proposed by Inoue [9] for application to penetrative materials.

#### Acknowledgements

We are grateful to Professor A. Drobnik for constant encouragement and also to Professor P. Klemm for the PCM samples and helpful discussions.

#### References

1. T. W. WOJTATOWICZ and K. ROŻNIAKOWSKI, in "Thermal conductivity", Vol. 20, edited by D. P. H. Hasselman and J. R. Thomas Jr. (Plenum Press, New York, 1987) p. 367.
2. H. S. CARSLAW and J. C. JAEGER, in "Conduction of heat in solids", (Oxford University Press, Oxford 1959) p. 283.
3. A. G. LANE, in "Solar heat storage, latent heat materials", Vol. 1, (CRC Press, Boca Raton, Florida, 1983).
4. R. C. F. SHAAKE, J. C. VAN MITENBURG and C. G. DE KRUIF, *J. Chem. Thermodyn.* **14** (1982) 771.
5. W. BARTCZAK, A. DROBNIK, P. KLEMM, A. KOTODZIEJSKI, K. ROŻNIAKOWSKI and T. W. WOJTATOWICZ, in Proceedings of the IMEKO Symposium on Microprocessors in Temperature and Thermal Measurement, Łódź, 16–18 May 1989, (Wydawnictwo Poltechniki, Łódzkiej, 1989) p. 155.
6. "Modelowanie numeryczne pól temperatury", edited by J. Szargut (WNT, Warszawa, 1992) p. 128 (in Polish).
7. S. Y. SUH and D. L. ANDERSON, *Appl. Optics* **23** (1984) 3965.
8. A. ROMANOWSKA and M. JABŁOŃSKI, in "Fizyka materiałów i konstrukcji budowlanych. Tom 3. materiały kompozytowe", edited by P. Klemm (Technical Univ. of Lodz, Lodz, 1995) p. 126 (in Polish).
9. K. INOUE, *High Temp. Technol.* **8** (1990) 21.

Received 6 February  
and accepted 3 October 1996